

COMPACT DUAL-BAND PRINTED DIVERSITY ANTENNA FOR WIMAX/WLAN APPLICATIONS

L. Xiong* and P. Gao

Research Institute of Electronic Science and Technology, University of Electronic Science and Technology of China, Chengdu 611731, China

Abstract—A compact dual-band multiple-input-multiple-output (MIMO)/diversity antenna is proposed. This antenna is designed for 2.4/5.2/5.8 GHz WLAN and 2.5/3.5/5.5 GHz WiMAX applications in portable mobile devices. It consists of two back-to-back monopole antennas connected with a T-shaped stub, where two rectangular slots are cut from the ground, which significantly reduces the mutual coupling between the two ports at the lower frequency band. The volume of this antenna is 40 mm * 30 mm * 1 mm including the ground plane. Measured results show the isolation is better than -20 dB at the lower frequency band from 2.39 to 3.75 GHz and -25 dB at the higher frequency band from 5.03 to 7 GHz, respectively. Moreover, acceptable radiation patterns, antenna gain, and envelope correlation coefficient are obtained. These characteristics indicate that the proposed antenna is suitable for some portable MIMO/diversity equipments.

1. INTRODUCTION

The enormous data requirement at anytime and anyplace has urged wireless communication systems such as wireless local area networks (WLAN) and worldwide interoperability for microwave access (WiMAX) to be widely studied and implemented. Multipath fading is a serious problem especially in urban and suburban environment which will degrade the system performance. The use of multiple-input-multiple-output (MIMO) technology is an effective way to improve the data rate and increase the channel capacity without sacrificing additional spectrum or transmitted power in a rich scattering environment [1–5]. Low mutual coupling between different ports of the multiple antennas is a pivotal to realize good performance of a MIMO

Received 30 June 2012, Accepted 30 August 2012, Scheduled 11 September 2012

* Corresponding author: Ling Xiong (xiaoxionguestc@yeah.net).

system. Too high mutual coupling will increase the signal correlation between the channels and decrease the antenna radiation efficiency [6].

It seems obvious that high port-to-port isolation will be ensured if the two radiating elements are spaced as far as possible. However, this is not a solution for mobile device with limited space. Thus, integrating multiple antennas closely in a small and compact mobile device while maintaining good isolation between them is a challenging task. A lot of efforts have been made to reduce the mutual coupling or enhance the isolation between closely placed antenna elements [7–16]. Decoupling networks for enhancing the port isolation between two closely spaced antennas are presented in [6, 7]. Though good isolation is obtained by using these methods, they make the antenna complex and increase the cost of manufacture. Various ground branches such as T-shaped branch [8–10], vertical branch [11], dual inverted L-shaped branches [12], tree-like structure branches [13] are applied to achieve high isolation. By linking two planar inverted F antennas (PIFAs) with a suspended strip to cancel the reactive coupling, the isolation between them can be improved [14–16]. Then, this method is further used on a printed microstrip antenna array for mobile applications [17–20]. High port isolation can also be achieved by etching slits or slots on the ground plane [21–25]. It is noticed that none of these antennas mentioned above are designed for both the 2.4/5.2/5.8 GHz WLAN bands and 2.5/3.5/5.5 GHz WiMAX bands. In [26], the authors present a wideband MIMO antenna with two novel bent slits which can cover the 2.4 to 6.55 GHz frequency band with good isolation. However, in this design, there is no interference suppression of nearby communication systems and thus affects the system performance. A dual-band MIMO antenna is proposed in [27]. It can not only operate at the whole WLAN and WiMAX bands but also cover the DCS-1800, PCS-1900, IMT-2000/UMTS systems, whereas the isolation of the 1.62 to 3.6 GHz band is just less than -13 dB which is not enough to achieve good diversity performance. This motivates us to design a dual-band MIMO antenna with good isolation for the WLAN and WiMAX applications.

In this paper, a dual-band MIMO antenna array is presented. The MIMO antenna array consists of two monopoles with back-to-back separation of nearly $0.058\lambda_0$ at 2.4 GHz. By connecting the two antennas with a T-shaped stub and cutting two rectangular slots from the ground plane, the isolation between the two ports is improved. Both simulated and measured results, including the S -parameters, radiation patterns, antenna gain and envelope correlation coefficient are reported. Details of the MIMO antenna array design is proposed and discussed.

2. ANTENNA DESIGN

The geometry and photograph of the proposed antenna are shown in Figures 1 and 2, respectively. The antenna system comprising two monopoles is fabricated on a low-cost FR-4 substrate with relative permittivity of 4.4 and thickness of 1 mm. Each of the monopoles is fed by a $50\ \Omega$ microstrip line. The L-shaped slot etched in the rectangular patch can make it produce extra resonant modes, thus widen the impedance bandwidth. A metal T-shaped stub which can reduce the mutual coupling caused by near-field is placed between the two monopoles. Two rectangles with height $h_3 = 4\text{ mm}$ and width $w_1 = 2.1\text{ mm}$ are cut from the ground plane to change the surface

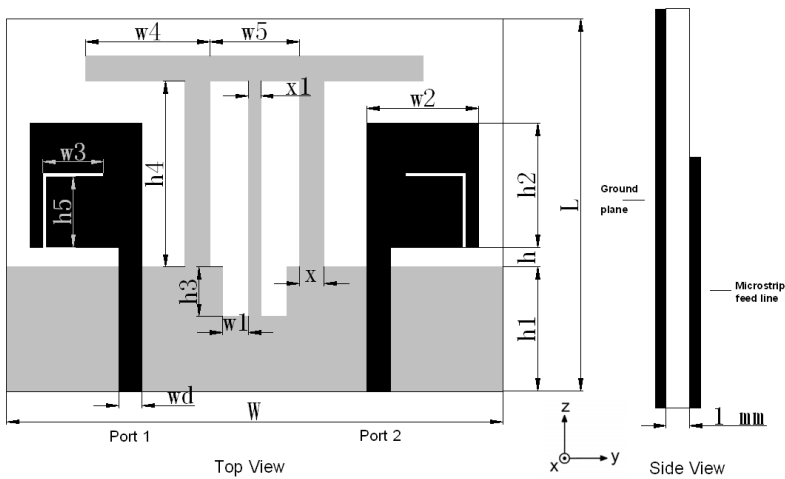


Figure 1. Geometry of the proposed antenna.

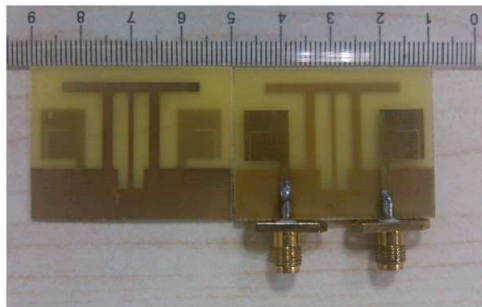
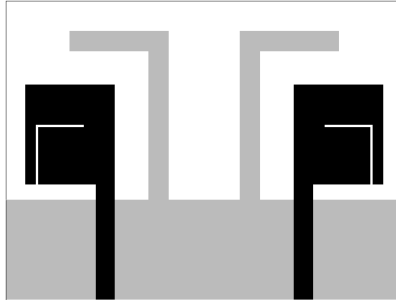


Figure 2. Photograph of the proposed antenna.

Table 1. Optimal parameters of the proposed antenna (see Figure 1).

Parameter	W	L	wd	w_1	w_2	w_3	w_4	w_5
Value (mm)	40	30	1.9	2.1	9	4.9	10	7.2
Parameter	x	x_1	h	h_1	h_2	h_3	h_4	h_5
Value (mm)	2	1	1.6	10	10	4	15	5.7

**Figure 3.** The geometry of the antenna without the decoupling structure (reference antenna).

current distribution on the ground plane. The proposed antenna is designed and analyzed by using the simulation software Ansoft HFSS V12. The optimal dimensions of the proposed antenna are shown in Table 1.

3. ANALYSIS OF WORKING MECHANISM

To analyze the effect of the mutual decoupling structure (include the T-shaped stub and two rectangular slots), another configuration will be investigated in this part. The antenna without the decoupling structure is called the reference antenna. Figure 3 shows the geometry of the reference antenna. The S -parameters of the two antennas are shown in Figures 4(a) and (b). It can be seen that the introduce of decoupling structure makes the reflection coefficient better at the lower frequency band and improves the isolation at 2.6 GHz from -12.7 dB to -17.9 dB. The isolation at the higher frequency band decreases because of the introducing of decoupling structure. However, it is not a problem for the isolation is still under -20 dB. There are two reasons which may increase the mutual coupling. One is the near-filed coupling caused by too close space, the other is the surface coupling caused by sharing the same ground plane. The T-shaped stub in this design is composed of a

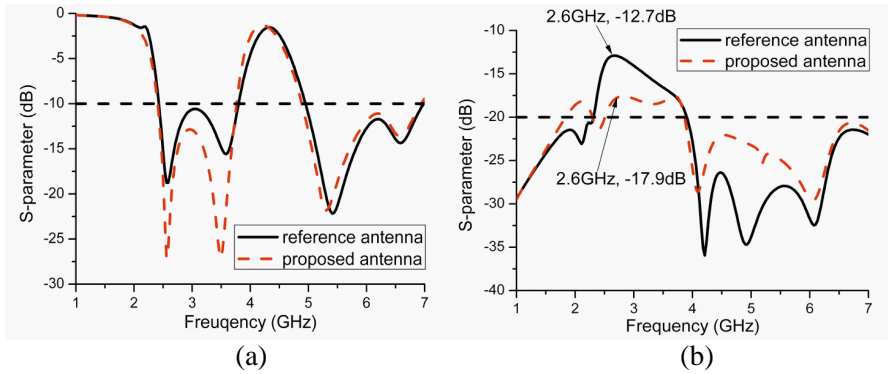


Figure 4. Simulated S -parameters of MIMO antenna with and without decoupling structure: (a) S_{11} , (b) S_{21} .

neutralization line and a vertical strip. The neutralization line provides an anti-phase coupling current to eliminate the original coupling route. This can reduce the electromagnetic coupling between two closely placed antennas [15, 20]. The vertical stub can be viewed as a reflector which can reduce the mutual coupling by separating the two antennas' radiation patterns [13, 27]. The two rectangular slots cut on the ground plane change the current distribution which further decreases the mutual coupling [23]. Figure 5 shows the simulated surface current distribution of the antenna with and without the decoupling structure. As it is seen, when port 1 is excited and port 2 is terminated with $50\ \Omega$, without the decoupling structure, much current flows from monopole 1 to monopole 2. Obviously, less current flows from monopole 1 to monopole 2 after the decoupling structure is added. It indicates that the decoupling structure can reduce the mutual coupling effectively. It has the same effect when port 2 is excited.

The function of the L-shaped strip and the L-shaped slot will be investigated in the next. Figure 6 shows the S -parameters of the reference antenna with and without the L-shaped strip. The L-shaped stripline provides the longest current route to generate the first resonant mode at 2.57 GHz. The length of the L-shaped strip is $h_4 + w_4 = 25\ \text{mm}$, which is about $\lambda/4$ at 2.57 GHz. Without the L-shaped stripline, the first resonant mode will vanish as shown in Figure 6(a). The L-shaped stripline also works as a reflector to reduce the mutual coupling caused by near-filed as show in Figure 6(b).

Figure 7 shows S -parameters of the reference antenna with and without the L-shaped slot. When the L-shaped slot is etched, two different current paths on the radiation patch can be obtained which

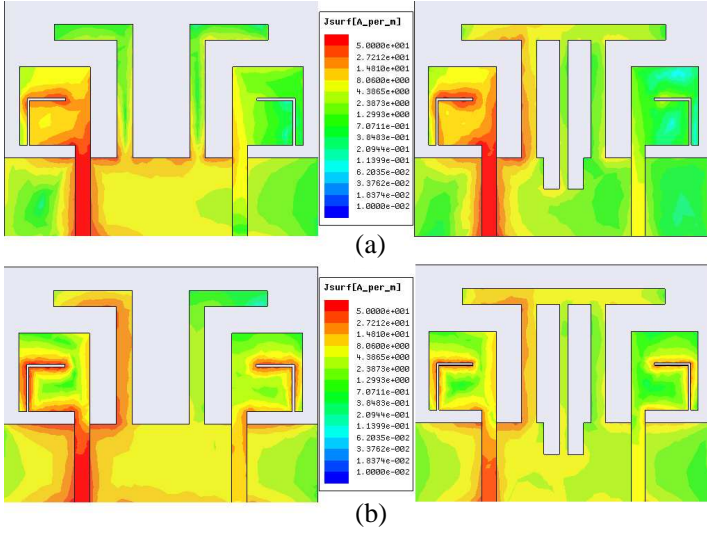


Figure 5. Current distribution of the MIMO antenna array when port 1 is excited: (a) 2.4 GHz, (b) 3.5 GHz.

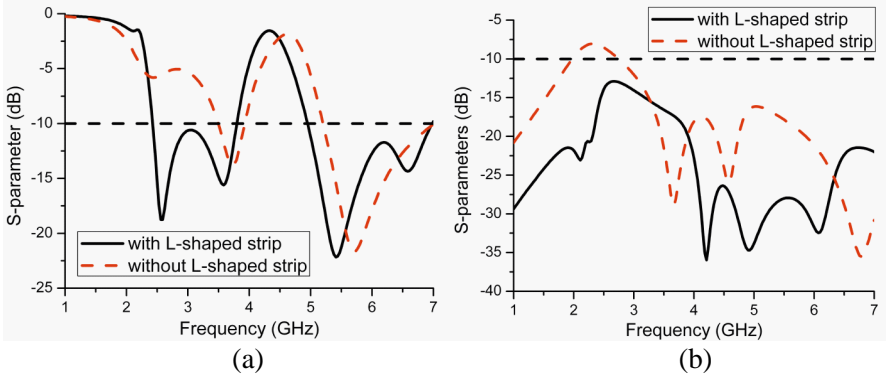


Figure 6. Simulated S -parameters of the reference antenna with and without L-shaped strip: (a) S_{11} , (b) S_{21} .

correspond to two resonant modes at 3.57 and 5.6 GHz, respectively. Then the dual-band characteristic can be obtained. The introduction of the L-shaped slot almost not affects the isolation between the two ports.

According to the above analysis, we investigated the parameters affect the impedance matching condition and isolation of the proposed

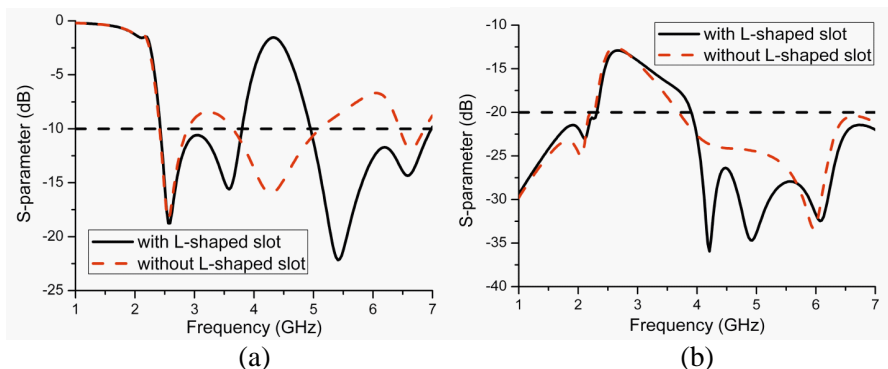


Figure 7. Simulated S -parameters of the reference antenna with and without L-shaped slot: (a) S_{11} , (b) S_{21} .

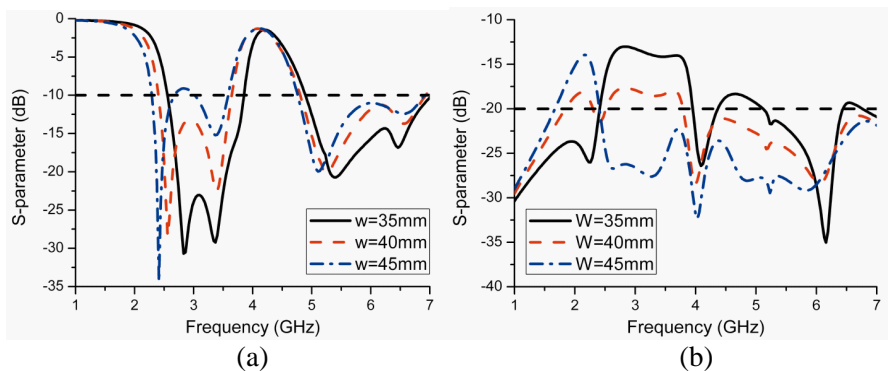


Figure 8. Simulated S -parameters of the proposed antenna with different values of W : (a) S_{11} , (b) S_{21} .

antenna most. Figure 8 shows the simulated S -parameters when the length of the proposed antenna W changes. It is found that the S_{21} in the frequency band 2.4–7 GHz decrease when W increase from 35 mm to 45 mm. However, with the increase of the W , the impedance matching condition in the lower frequency band 2.4–3.7 GHz becomes worse. Figure 9 plots the simulated S -parameters when the height of the L-shaped strip h_4 varies from 15 mm to 19 mm. Too long h_4 will make the impedance matching condition at the lower frequency band worse, while too short h_4 will deteriorate the S_{21} in the lower frequency band. Figure 10 illustrates the simulated S -parameters for different values of h_5 . It can be clearly seen that with the increase of the h_5 the second and third resonant modes shift to lower frequency band. Small effects are found on the isolation when h_5 changes.

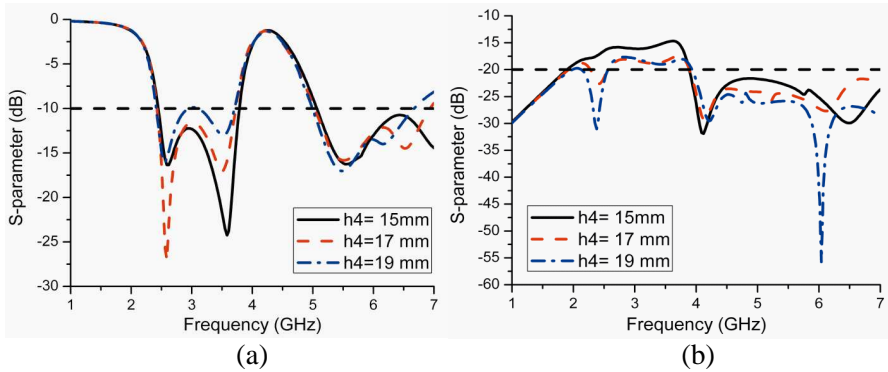


Figure 9. Simulated S -parameters of the proposed antenna with different values of h_4 : (a) S_{11} , (b) S_{21} .

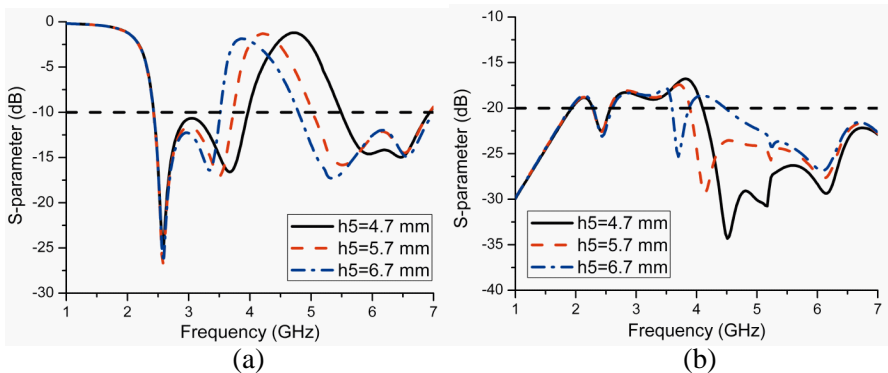


Figure 10. Simulated S -parameters of the proposed antenna with different values of h_5 : (a) S_{11} , (b) S_{21} .

4. RESULTS AND DISCUSSIONS

To validate the simulated results, the proposed MIMO antenna shown in Figure 1 has been fabricated and tested. The S -parameters of the antenna are measured by Agilent E8363B vector network analyzer (VNA). The measured and simulated S -parameters are plotted in Figure 11. As can be seen, the impedance bandwidths for $S_{11} \leq -10$ dB are about 1360 MHz (from 2.39 GHz to 3.75 GHz) with $S_{21} \leq -20$ dB and 1970 MHz (from 5.03 GHz to 7 GHz) with $S_{21} \leq -25$ dB, which can cover the 2.4–2.484, 5.15–5.35, and 5.725–5.825 GHz WLAN bands and the 2.5–2.69, 3.4–3.69, and 5.25–5.85 GHz WiMAX bands.

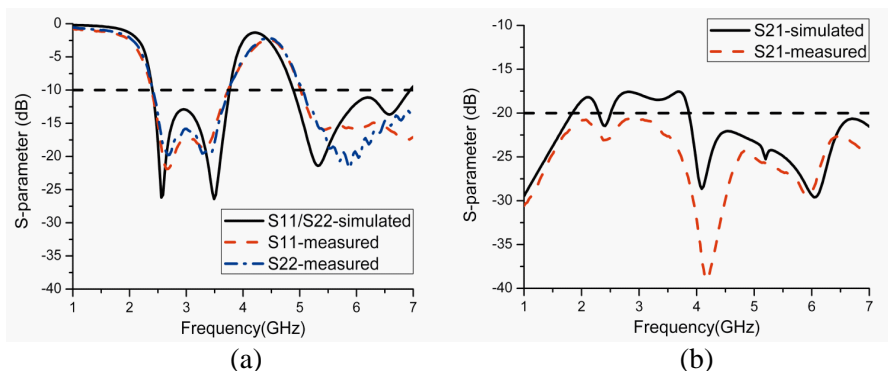


Figure 11. Simulated and measured S -parameters of the proposed antenna: (a) S_{11} and S_{22} , (b) S_{21} .

There is a small discrepancy between the simulated and measured S -parameters for the reason of mismatch between the SMA connector and the antenna feedline.

The radiation patterns of the proposed antenna are measured and simulated at three frequencies 2.4, 3.5 and 5.5 GHz and shown in Figure 12. During the measurement and simulation, the Port 1 is excited, while the Port 2 is terminated with a 50-Ω load. The total efficiency of an antenna is defined as the total radiated power divided by the incident power at the feed. The factors for the loss of efficiency are dielectric loss of the FR4 substrate, ohmic losses in all the metallic parts, and the reflection losses due to the mismatch between the co-axial probe and the antenna. In a two-port antenna system, the isolation between the two ports should also take into account, because if any energy input at one port can exit through another port, that energy will be dissipated in its terminal load. The following equations can be used to calculate the respective total efficiency of the two ports [15]:

$$\eta_{total1} = \eta_{rad1} \left(1 - |S_{11}|^2 - |S_{21}|^2 \right) \tag{1}$$

$$\eta_{total2} = \eta_{rad2} \left(1 - |S_{22}|^2 - |S_{12}|^2 \right) \tag{2}$$

η_{rad1} and η_{rad2} are the radiation efficiencies of the port 1 and port 2. Figure 13 plots the measured peak gain and calculated total efficiency of the reference and proposed antennas when Port 1 is excited. Because of the symmetrical structure, only the gain and total efficiency of one of the two ports are presented. It can be seen that in the lower frequency band from 2.4 GHz to 3.7 GHz the efficiency of the proposed antenna is larger than the reference antenna. This is because in this working

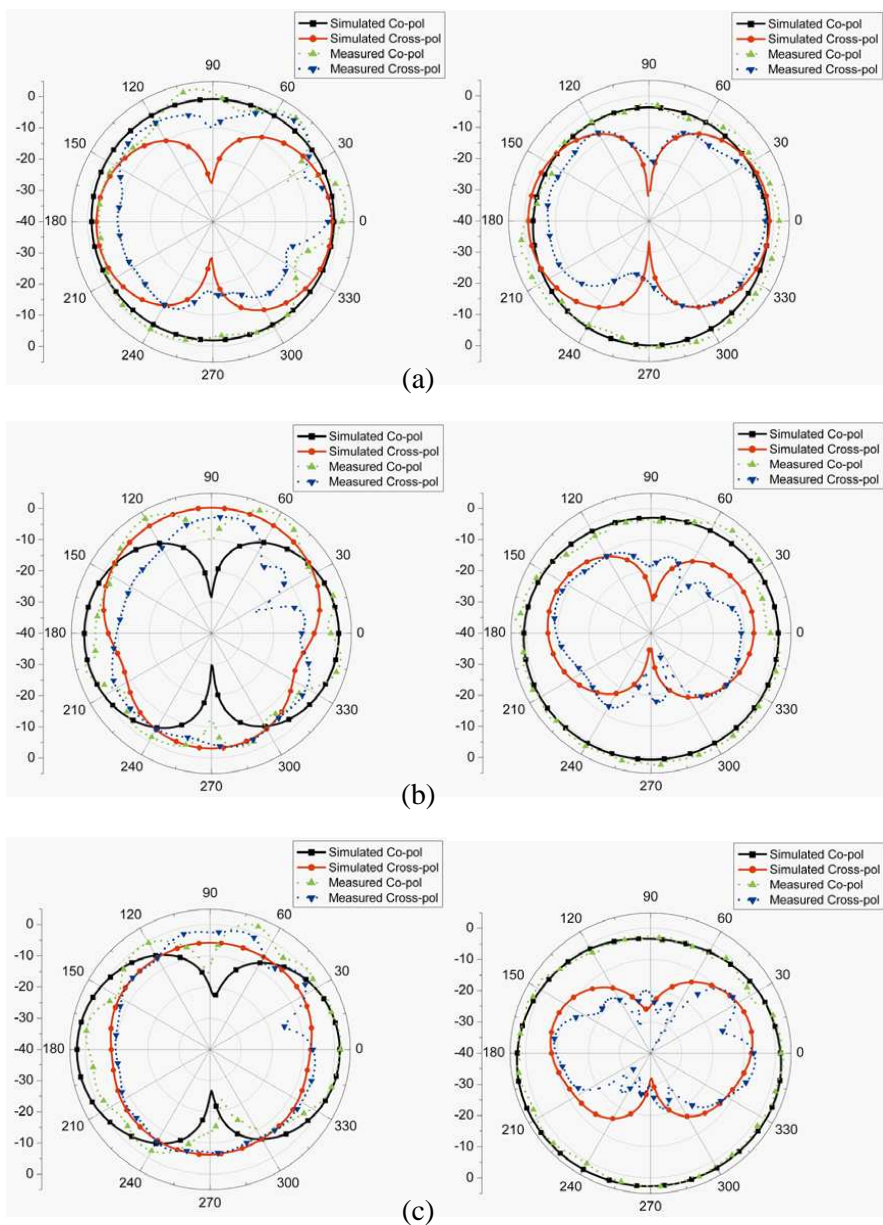


Figure 12. Radiation patterns of the proposed antenna for two planes (left: $x-z$ plane, right: $x-y$ plane) at (a) 2.4 GHz, (b) 3.5 GHz, and (c) 5.5 GHz.

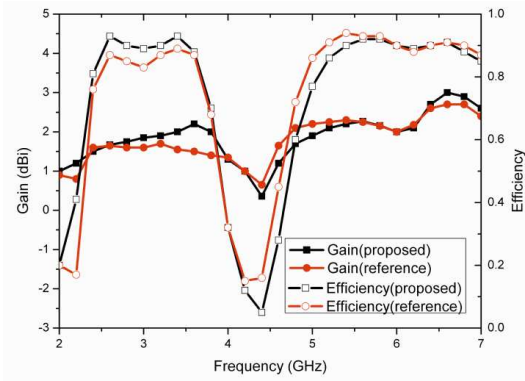


Figure 13. The measured peak gain and calculated total efficiency of the reference and proposed antennas when Port 1 is excited.

band the isolation of the proposed antenna is much better than the reference antenna, which makes less energy at Port 1 of the antenna leaks to Port 2. Thus, more energy can be radiated from Port 1. For the same reason, the efficiency of the reference antenna is larger than the proposed antenna in the higher frequency from 4.2 GHz to 6 GHz. The peak gain in the lower frequency band varies from 1.5 dBi to 2.2 dBi with an average of 1.86 dBi, and the radiation efficiency is larger than about 76%. In the higher frequency band, the peak gain changes from 2 dBi to 3 dBi with an average of 2.4 dBi, and the radiation efficiency is larger than about 86%.

The envelope correlation coefficient (ECC) is an important parameter to evaluate the MIMO/diversity performance of the antenna. It can be employed to estimate the degree of similarity between the two beam patterns. Generally, low envelope correlation may mean less overlapping between the two beam patterns. The envelope correlation coefficient can be calculated by using S -parameters or radiation patterns which are described in detail in [28] and [12, 15, 29, 30], respectively. Here, the correlation coefficient, ρ_{eij} , between the i th and j th elements ($i, j = 1$ to n , where n is the total number of antenna elements) is calculated through the complex correlation coefficient ρ_{cij} as shown in Equation (3) [29]:

$$\rho_{eij} = |\rho_{cij}|^2 = \left| \frac{\int_0^{2\pi} A_{ij}(\phi) d\phi}{\sqrt{\int_0^{2\pi} A_{ii}(\phi) d\phi \int_0^{2\pi} A_{jj}(\phi) d\phi}} \right|^2 \quad (3)$$

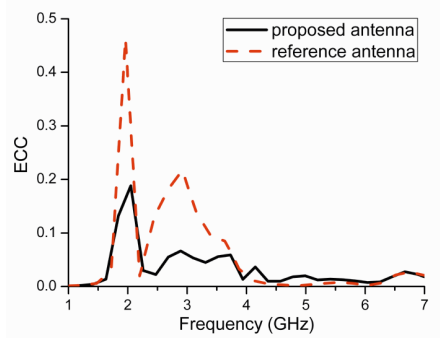


Figure 14. The calculated envelope correlation coefficient (ECC) of the reference and proposed antennas.

where

$$A_{ij}(\phi) = \Gamma E_{\theta i}(\pi/2, \phi) E_{\theta j}^*(\pi/2, \phi) + E_{\phi i}(\pi/2, \phi) E_{\phi j}^*(\pi/2, \phi)$$

in which

$$\vec{E}_p(\theta, \phi) = E_{\theta p}(\theta, \phi) \vec{\theta} + E_{\phi p}(\theta, \phi) \vec{\phi}$$

is the vector radiation pattern associated with antenna # p . Γ is the cross-polarization discrimination (XPD) (ratio of vertical to horizontal electric field strength) of the incident field. In this paper, Γ is chosen as 0 dB which is the average in an indoor environment [1]. The Equation (3) is based on the condition that the fading envelope being Rayleigh distributed, the incoming field arriving in the horizontal plane only, the incoming field's orthogonal polarizations being uncorrelated, the individual polarizations being spatially uncorrelated, and finally the time-averaged power density per steradian is constant [29, 30]. Figure 14 presents the calculated envelope correlation coefficient of the reference and proposed antennas. From the figure, it can be concluded that the ECC of the proposed antenna is much smaller than the reference antenna at the lower frequency band 2.4–3.7 GHz. Moreover, the ECC of the proposed antenna is less than 0.1 in the whole working band which satisfies the MIMO requirement for $\rho_{eij} \leq 0.5$ [1].

5. CONCLUSION

A low-profile dual-band MIMO/diversity antenna system has been investigated in this paper. The measured impedance bandwidth for $S_{11} \leq -10$ dB varies from 2.39 GHz to 3.75 GHz and 5.03 GHz to 7 GHz with isolation below -20 dB and -25 dB, respectively. The high isolation performance is obtained by connecting the two monopoles with a T-shaped stub and etching two rectangular slots on the ground

plane. The radiation patterns, antenna gain, efficiency and envelope correlation coefficient have also been simulated and calculated. The calculated envelope correlation efficiency of the proposed MIMO antenna in the working band is less than 0.02. These results show that the proposed antenna system is suitable for portable MIMO/diversity applications.

ACKNOWLEDGMENT

This work is supported by the Fundamental Research Funds for the Central Universities of China (No. ZYGX2010J117).

REFERENCES

1. Vaughan, R. G. and J. B. Andersen, "Antenna diversity in mobile communications," *IEEE Transactions on Vehicular Technology*, Vol. 36, No. 4, 149–172, 1987.
2. Foschini, G. J. and M. J. Gans, "On limits of wireless communications in a fading environment when using multiple antennas," *Wireless Personal Communication*, Vol. 6, 311–335, 1998.
3. Abouda, A. A. and S. G. Hggman, "Effect of mutual coupling on capacity of MIMO wireless channels in high SNR scenario," *Progress In Electromagnetics Research*, Vol. 65, 27–40, 2006.
4. Bolin, T., A. Derneryd, G. Kristensson, V. Plicanic, and Z. Ying, "Two-antenna receive diversity performance in indoor environment," *Electronic Letters*, Vol. 41, 1205–1206, 2005.
5. Boerman, J. D. and J. T. Bernhard, "Performance study of pattern reconfigurable antennas in MIMO communication systems," *IEEE Transactions on Antennas and Propagation*, Vol. 56, No. 1, 231–236, 2008.
6. Chen, S.-C., Y.-S. Wang, and S.-J. Chung, "A decoupling technique for increasing the port isolation between two strongly coupled antennas," *IEEE Transactions on Antennas and Propagation*, Vol. 56, No. 12, 3650–3658, 2008.
7. Cui, S., S. X. Gong, Y. Liu, W. Jiang, and Y. Guan, "Compact and low coupled monopole antennas for MIMO system applications," *Journal of Electromagnetic Waves and Applications*, Vol. 25, Nos. 5–6, 703–712, 2011.
8. Chi, G., B. Li, and D. Qi, "Dual-band printed diversity antenna for 2.4/5.2 GHz WLAN application," *Microwave and Optical Technology Letters*, Vol. 45, No. 6, 561–563, 2005.

9. Wu, T.-Y., S.-T. Fang, and K.-L. Wong, "Printed diversity monopole antenna for WLAN operation," *Electronic Letters*, Vol. 38, No. 25, 1625–1626, 2002.
10. Cheng, Y., W.-J. Lü, C.-H. Cheng, W. Cao, and Y. Li, "Compact diversity antenna with T shape stub for ultra-wideband applications," *Proc. 2008 Asia-Pacific Microwave Conference*, 1–4, Macau, 2008.
11. See, T. S. P. and Z. N. Chen, "An ultrawideband diversity antenna," *IEEE Transactions on Antennas and Propagation*, Vol. 57, No. 6, 1597–1604, 2009.
12. Ding, Y., Z. Du, K. Gong, and Z. Feng, "A novel dual-band printed diversity antenna for mobile terminals," *IEEE Transactions on Antennas and Propagation*, Vol. 55, No. 7, 2088–2096, 2007.
13. Zhang, S., Z. Ying, J. Xiong, and S. He, "Ultrawideband MIMO/diversity antennas with a tree-like structure to enhance wideband isolation," *IEEE Antennas and Wireless Propagation Letters*, Vol. 8, 1279–1283, 2009.
14. Diallo, A., C. Luxey, P. L. Thuc, R. Staraj, and G. Kossiavas, "Study and reduction of the mutual coupling between two mobile phone PIFAs operating in the DCS1800 and UMTS bands," *IEEE Transactions on Antennas and Propagation*, Vol. 54, No. 11, 3063–3073, 2006.
15. Diallo, A., C. Luxey, P. Le Thuc, R. Staraj, and G. Kossiavas, "Enhanced two-antenna structures for universal mobile telecommunications system diversity terminals," *IET Microwave Antennas and Propagation*, Vol. 2, 93–101, 2008.
16. Chebihi, A., C. Luxey, A. Diallo, P. L. Thuc, and R. Staraj, "A novel isolation technique for closely spaced PIFAs for UMTS mobile phones," *IEEE Antennas Wireless Propagation Letters*, Vol. 7, 665–668, 2008.
17. Li, Z., K. Ito, Z. Du, and K. Gong, "Compact wideband printed diversity antenna for mobile handsets," *Proc. 2010 Asia-Pacific Radio Science Conference*, 1–4, Toyama, Japan, 2010.
18. Ling, X. and R. L. Li, "A novel dual-band MIMO antenna array with low mutual coupling for portable wireless devices," *IEEE Antennas Wireless Propagation Letters*, Vol. 10, 1039–1042, 2008.
19. Su, S.-W., C.-T. Lee, and F.-S. Chang, "Printed MIMO-antenna system using neutralization-line technique for wireless USB-dongle applications," *IEEE Transactions on Antennas and Propagation*, Vol. 60, No. 2, 456–463, 2012.

20. See, C. H., R. A. Abd-Alhameed, Z. Z. Abidin, N. J. McEwan, and P. S. Excell, "Wideband printed MIMO/diversity monopole antenna for WiFi/WiMAX applications," *IEEE Transactions on Antennas and Propagation*, Vol. 60, No. 4, 2028–2035, 2012.
21. Tounou, C., C. Decroze, D. Carsenat, T. Monédière, and B. Jécko, "Diversity antennas efficiencies enhancement," *Proc. IEEE Antennas Propagation International Symposium*, 1064–1067, Honolulu, HI, 2007.
22. Kim, I., C. W. Jung, Y. Kim, and Y. E. Kim, "Low-profile wideband MIMO antenna with suppressed mutual coupling between two antennas," *Microwave and Optical Technology Letters*, Vol. 50, No. 5, 1336–1339, 2008.
23. Chou, H.-T., H.-C. Cheng, H.-T. Hsu, and L.-R. Kuo, "Investigations of isolation improvement techniques for multiple input multiple output (MIMO) WLAN portable terminal applications," *Progress In Electromagnetics Research*, Vol. 85, 349–366, 2008.
24. Zuo, S., Y.-Z. Yin, W.-J. Wu, Z.-Y. Zhang, and J. Ma, "Investigations of reduction of mutual coupling between two planar monopoles using two $\lambda/4$ slots," *Progress In Electromagnetics Research Letters*, Vol. 19, 9–18, 2010.
25. Cui, S., Y. Liu, W. Jiang, S. X. Gong, Y. Guan, and S. T. Yu, "A novel compact dual-band MIMO antenna with high port isolation," *Journal of Electromagnetic Waves and Applications*, Vol. 25, Nos. 11–12, 1645–1655, 2011.
26. Li, J.-F., Q.-X. Chu, and T.-G. Huang, "A compact wideband MIMO antenna with two novel bent slits," *IEEE Transactions on Antennas and Propagation*, Vol. 60, No. 2, 482–489, 2012.
27. Li, J.-F. and Q.-X. Chu, "A compact dual-band MIMO antenna of mobile phone," *Journal of Electromagnetic Waves and Applications*, Vol. 25, Nos. 11–12, 1577–1586, 2011.
28. Blanch, S., J. Romeu, and I. Corbella, "Exact representation of antenna system diversity performance from input parameter description," *Electronic Letters*, Vol. 39, No. 9, 705–707, 2003.
29. Jensen, M. A. and Y. Rahmat-Sei, "Performance analysis of antennas for hand-held transceivers using FDTD," *IEEE Transactions on Antennas and Propagation*, Vol. 42, No. 8, 1106–1113, 1994.
30. Ko, S. C. K. and R. D. Murch, "Compact integrated diversity antenna for wireless communications," *IEEE Transactions on Antennas and Propagation*, Vol. 49, No. 6, 954–960, 2001.